Renewable Energy 81 (2015) 543–550

Contents lists available at ScienceDirect

Renewable Energy

journal homepage: www.elsevier.com/locate/renene

Analysis and enhancement of PV efficiency with incremental conductance MPPT technique under non-linear loading conditions

P. Sivakumar [a], Abdullah Abdul Kader [a, *], Yogeshraj Kaliavaradhan [a], M. Arutchelvi [b]

[a] Department of Electrical &Electronics, J.J College of Engineering and Technology, Tamilnadu, India
[b] Department of Electrical & Electronics, Saranathan College of Engineering and Technology, Tamilnadu, India

ARTICLE INFO

Article history:
Received 26 March 2014
Accepted 22 March 2015
Available online

Keywords:
Maximum power point tracking (MPPT)
Incremental conductance(IC)
Non-linear load
Photovoltaic (PV)
MATLAB-Simulink

ABSTRACT

This paper presents experimental evaluations for variation in the efficiency of energy extracted from a photovoltaic (PV) module (under non-linear loading) incorporated with an incremental conductance(IC) maximum power point tracking (MPPT) algorithm. The focus is on the evaluation of the PV panel under non-linear loading conditions using the experimental installation of a 100W_p photovoltaic array connected to a DC–DC converter and a KVA inverter feeding a non-linear load. Under the conditions of non-linear loading, both the simulation and experiment show that the MPPT technique fails to attain maximum power point due to the presence of ripples in the current leading eventually to a reduction in efficiency. In this paper, panel current is taken as a function of load impedance in the MPPT algorithm to eradicate power variation, as load impedance varies with supply voltage under non-linear conditions. The system is simulated for different non-linear loads using MATLAB-Simulink. A TMDSSOLAREXPKIT was used for MPPT control. In case 2, the inverter is connected to a single phase grid. When a voltage swell occurs in the grid, PV power drops. This power loss is reduced using the proposed MPPT method. The results of simulations and experimental measurements and cost efficiency calculations are presented.

1. Introduction

The growing demand in energy utilization and fast depleting natural resources like petroleum and coal have resulted in the threat of a major energy crises globally. Alternate energy resources can contribute a convincing amount of energy to overcome such energy crises. A commonly used alternate energy form is solar energy, which is a pure form of energy directly from sun [1,2], The photovoltaic (PV) which converts the solar energy into electrical energy, and an array of PV panels connected in series/parallel can energize certain loads. The solar irradiation from the sun is not constant, due to varying atmospheric conditions; resulting in varying voltage and current in the PV which eventually produces fluctuating power [3,4]. Consequently, an MPPT technique is indispensible for real time systems [5]. Many MPPT algorithms were proposed for a two stage and single stage grid connected system with some limitations in system performance. Comparisons of various MPPT technique like Perturb and observe, incremental conductance and soft computing methods are discussed in Refs. [6–8] and a survey energy reduction of the PV array with nonlinear load variations is not included. Most MPPT techniques are considered with constant output impedance or load impedance being connected to PV output terminals. These techniques are considered only the source (irradiations) variations or load variations only are observed by Ref. [9]. Most MPPT's are based on varying duty ratio and also continuously (like boost converter and its derived advanced versions) or discontinuously (buck and its derived advanced versions) connected to the power circuit. Effective impedance on both input and output terminals is not considered. The proposed method, a simple strategy to extract peak power from the grid connected PV with nonlinear load at PCC is attempted.

The proposed method has focused on the following points.

MPPT is achieved by regulating the effective conductance appropriately properly ($i^r_{pv}/v^r_{pv}$of the output terminal of PV array during nonlinear load). The effective conductance also takes into account the rate of change in conductance due to source, load and storage element nonlinearities. This effective change in conductance variable is added to earlier incremental conductance (impedance) variations due instantaneous non-linear loads. Further the change in conductance also considers voltage, current ripples and nonlinear loads to track MPP. In literature however the output impedance most of MPPT techniques are considered at constant loads. Furthermore, voltage swell and sag at PCC may

* Corresponding author. Department of Electrical & Electronics, J.J College of Engineering and Technology, Tamilnadu, India.
E-mail addresses: lpssivakumar@gmail.com (P. Sivakumar), abdul25792@gmail.com (A. Abdul Kader), yoge21raj@gmail.com (Y. Kaliavaradhan).

http://dx.doi.org/10.1016/j.renene.2015.03.062
0960-1481/

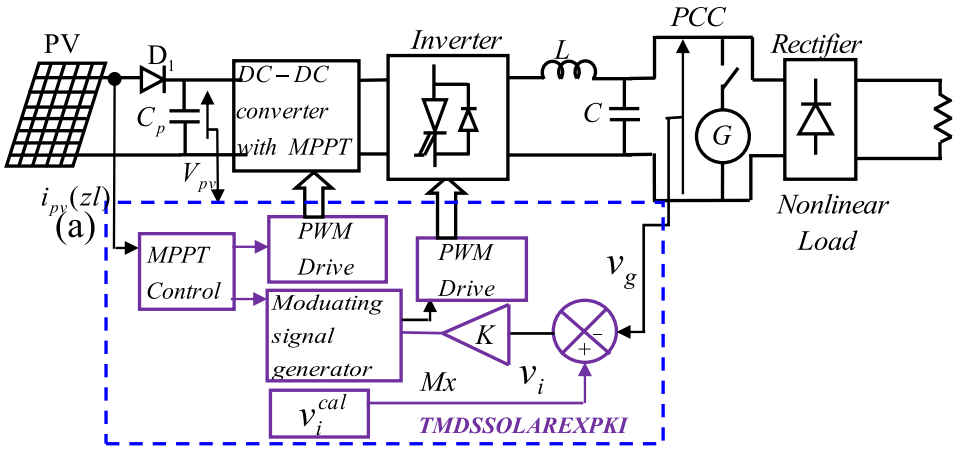

Fig. 1. Basic functional block diagram.

affect conventional MPPT techniques for single stage grid connected operations. But the proposed technique overcomes the above complications and thereby improves the energy extracted from PV MPPT.

New generation PV panels are incorporated with Maximum Power Point tracker (MPPT) which tracks the maximum voltage and current (V_{MPP} and I_{MPP}) to set the operating point at maximum power to operate at higher efficiency. This paper gives a detailed analysis of the voltage, current and efficiency of a PV operating at maximum power point when connected to a nonlinear load. The block diagram of the system shown in Fig. 1 is considered for the experiment, in this paper.

It is known that nonlinearity in the load condition affects the impedance of the system precisely. There are various MPPT technique like Perturb and observe, incremental conductance, fuzzy etc. These techniques are discussed by the authors in this work [10]. In this paper, incremental conductance MPPT is considered which makes the PV adjust its power to maximum power depending on conductance C and change in conductance [11]. Conductance C is an inverse of system impedance Z, so when the PV is loaded with nonlinear loads it fails to operate at maximum power varying effective impedance which varies conductance.

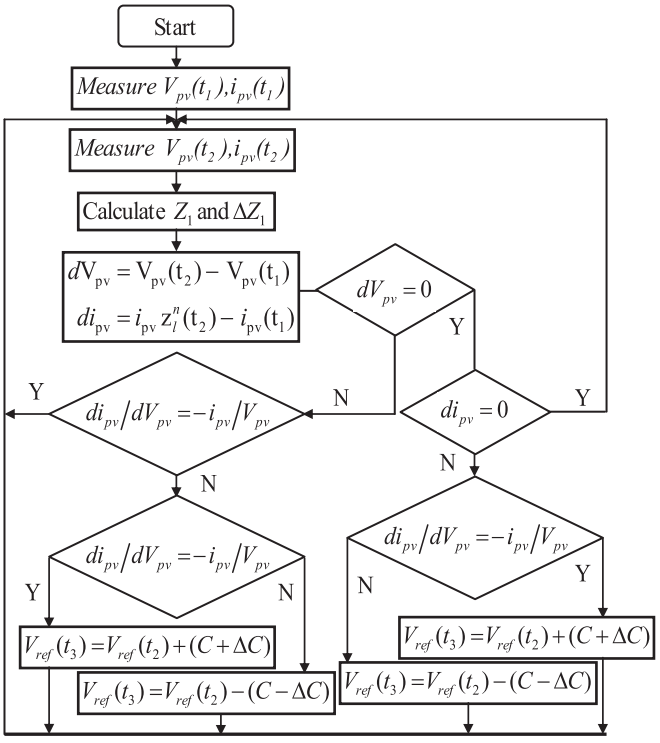

Fig. 2. Flowchart for incremental conductance MPPT.

1.1. Nonlinear loads

When the applied voltage provokes a change in the impedance of a load, it is considered to be non-linear. The change in impedance brings in non-linearity in the current drawn by the load even when connected to a sinusoidal voltage source. These non-sinusoidal currents contain harmonic currents that interact with the impedance of the power distribution system to create voltage distortions that affect the distribution system equipment and loads connected to it [12] Results of empirical studies proved that large non-linear loads are primary contributors to power system harmonics [13]. Alternatively, large scale production of small non-linear loads used as switching components, like transistors and diodes have the potential of aggravating harmonic distortion levels in commercial office buildings and in industrial applications [14]. Large non-linear loads are primarily contributed by electrical machines and drives, where power converters are combined with electric motors and electronic control circuits. Conversely, small non-linear loads are primarily contributed by active switches which respond to applied signal with turn on and turn off; and passive switches with a highly non-linear *v-i* characteristic. Reactive components like inductors and capacitors are sources of non-linearity. Additionally, the proliferation of multi-megawatt power converters in flexible ac transmission systems (FACTS) happens to be an anticipated challenge.

1.2. Effects of nonlinear loads

The increasing number of non-linear loads on typical commercial office buildings and distribution systems has made the

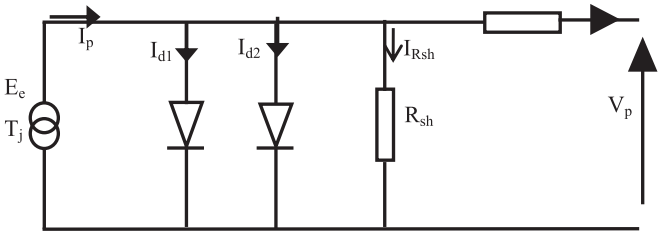

Fig. 3. Equivalent circuit for a two diode model.

presence of harmonics inevitable leading to the increase of waveform voltage and current supply distortions resulting in power quality issues. This necessitates the study of the non-linearity in power system as addressed by the authors in this work [15].

2. Incremental conductance MPPT

Incremental conductance technique is used extensively due to its high adaptability and accuracy even under changing atmospheric conditions [3]. It is based on power variations directly. The output voltage and output current from the PV panel are measured using sensors to calculate conductance ($C=I_p/V_p$) and incremental Effective conductance ($\Delta C = (\Delta I_p/\Delta V_p) + C_E$). The slope of the PV array power curve is zero at the MPP, positive on its left, and negative on the right. The flowchart for incremental conductance with a solution for a non-linear load is shown in Fig. 2.

The symbols in Fig. 2 are defined as V_p: panel voltage; I_p: panel current; Z_l: load impedance; $\Delta Z_l = (I_l/V_l + C_E)$: change in load impedance; $I_{p(Zl)}$: panel current as a function of load impedance; C: conductance; ΔC: change in conductance: $C_E = [I_l/V_l]^{St}$ change in Effective conductance: St switching cycle. The principle behind the technique is to compare the values of conductance and incremental conductance to decide whether to increase or decrease the PV voltage to reach the Maximum Power Point. As non-linear loads are considered, where the load impedance (Z_l) varies with supply voltage, PV panel current is taken as a function of load impedance.

dP/dV = 0, at Maximum Power Point
dP/dV > 0, to the left of Maximum Power Point
dP/dV < 0, to the right of Maximum Power Point.

The objective of this algorithm is to track the operating point of voltage, where conductance is equal to incremental conductance. Hence, the following equations,

$$\frac{dP_p}{dV_p} = 0 \frac{I_p}{V_p} = \frac{dI_p}{dV_p},\ C = \Delta C \tag{1}$$

$$\frac{dP_p}{dV_p} > 0 \frac{I_p}{V_p} > -\frac{dI_p}{dV_p},\ C > \Delta C \tag{2}$$

$$\frac{dP_p}{dV_p} < 0 \frac{I_p}{V_p} < -\frac{dI_p}{dV_p},\ C < \Delta C \tag{3}$$

When the point at which $C = \Delta C$ obtained, MPPT operates at that point till a further change in current occurs, which has a direct relation to the irradiance of the PV array. The panel current I_p as a function of load impedance is calculated as,

$$I_{p(Z_l)} = I_{ph} - I_s \left(\exp \frac{q(V_p + R_s I_p)}{AKT_j} \right) - 1 - \frac{V_p + R_s I_p}{R_{sh}} \pm Z_l \tag{4}$$

where, I_{ph} is the photo current, R_s is series resistance, R_{sh} is shunt resistance, A the diode ideality factor, K is Boltzman's constant ($K = 1.381 \times 10{-}23$ J/K) and T_j is junction temperature.

$$\frac{dI_p}{dV_p} = -\frac{1}{R_s + \left(\frac{1}{\frac{qI_s}{AKT_j} \exp \frac{q(V_p + R_s I_p)}{AKT_j}} \right) + \frac{1}{R_{sh}}} \pm \Delta Z_l \tag{5}$$

where, q is a quantum of charge. The mathematical equation for panel current as a function of load impedance and for incremental conductance is given by Eqs. (4) and (5) respectively.

3. Modeling of photovoltaic (PV) panel

A two diode model is taken for discussion, wherein the transport of electric charges inside the cell is considered [4]. The symbols in Fig. 3 are defined as I_{d1}: current across diode D1 and I_{d2}: current across diode D2. The panel current I_p can be written as,

$$I_p = I_{ph} - (I_{d1} + I_{d2}) - I_{Rsh} \tag{6}$$

where,

$$I_p = C_1 \cdot E_e \left[1 + C_2 \cdot \left(E_e - E_{e\ ref} \right) + C_3 \left(T_j - T_{ref} \right) \right] \tag{7}$$

In Eq. (7) V_p is the panel voltage,C_1, C_2 and C_3 are constant parameters; E_e: irradiance (W/m^2); T_{ref}: reference temperature 25 °C. The shunt current I_{Rsh} is given as,

$$I_{Rsh} = \left(\frac{V_p + R_s \cdot I_p}{R_{sh}} \right) \tag{8}$$

$$I_{d1} = I_{01} \cdot \left[\exp \frac{q(V_p + R_s I_p)}{n \cdot N_{cs} \cdot K \cdot T_j} \right) - 1 \tag{9}$$

$$I_{d2} = I_{02} \cdot \left[\exp \frac{q(V_p + R_s I_p)}{2 \cdot n \cdot N_{cs} \cdot K \cdot T_j} \right) - 1 \tag{10}$$

where, n is the diode ideality factor and N_{cs} are the number of cells in series. Saturation currents are stated as,

$$I_{01} = C_4 T_j^3 \exp \frac{-E_g}{K \cdot T_j} \tag{11}$$

$$I_{02} = C_5 T_j^3 \exp \frac{-E_g}{2 \cdot K \cdot T_j} \tag{12}$$

The expression for panel current after substitution is as follows.

$$I_p = C_1 \cdot E_g \cdot \left[1 + C_2 \cdot \left(E_e - E_{e\ ref} \right) + C_3 \cdot \left(T_j - T_{ref} \right) \right] - \left(\frac{V_p + R_s \cdot I_p}{R_{sh}} \right) - C_4 \cdot T_j^3 \cdot \exp \frac{-E_g}{k \cdot T_j} \cdot \left[\exp q \cdot \frac{(V_p + R_s I_p)}{n \cdot N_{cs} \cdot K \cdot T_j} \right) - 1 \Bigg] - C_5 \cdot T_j^3 \cdot \exp \frac{-E_g}{2 \cdot k \cdot T_j} \cdot \left[\exp q \cdot \frac{(V_p + R_s I_p)}{2 \cdot n \cdot N_{cs} \cdot K \cdot T_j} \right) - 1 \Bigg] \tag{13}$$

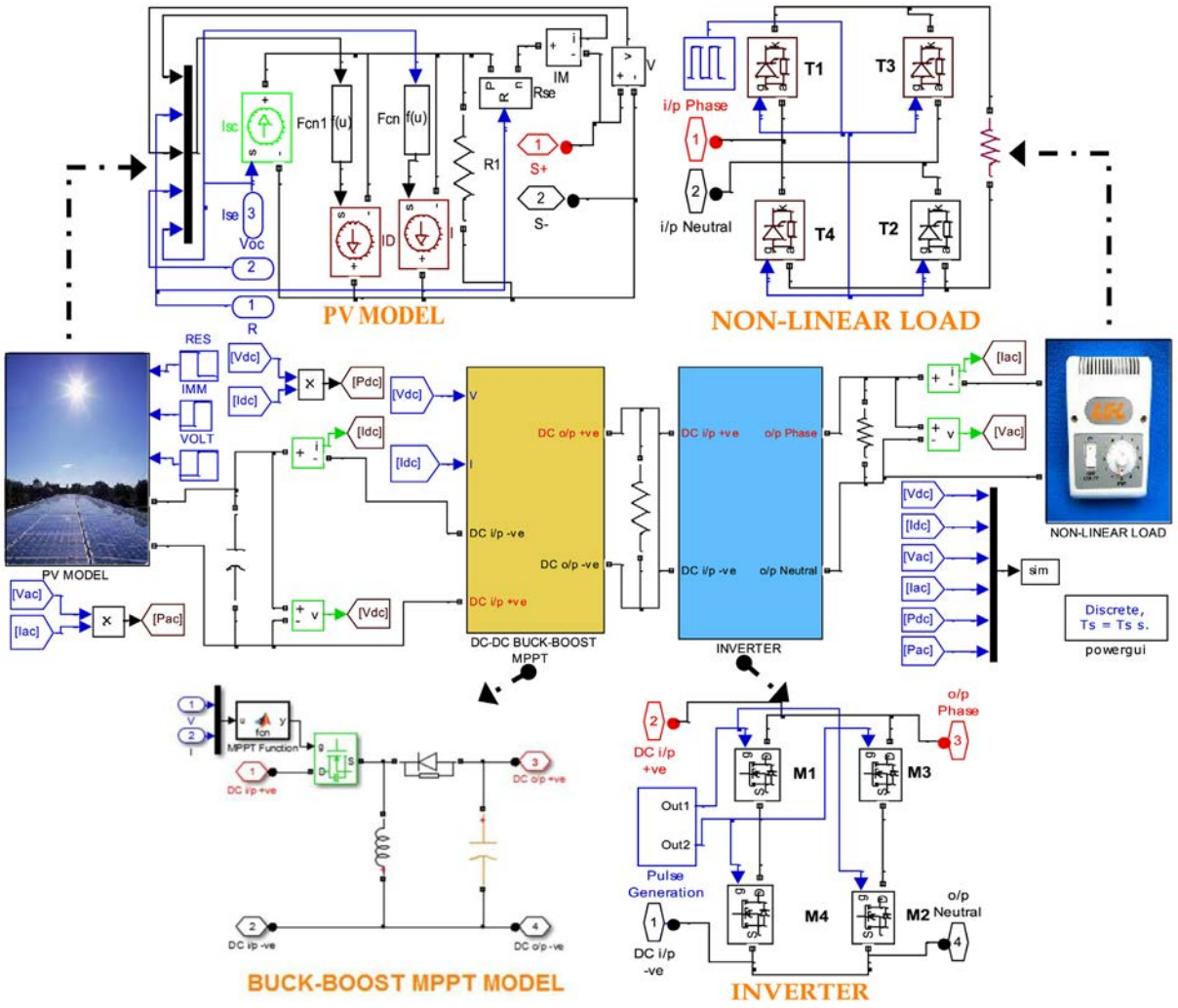

Fig. 4. The simulation circuit for the overall system with subsystems expanded individually.

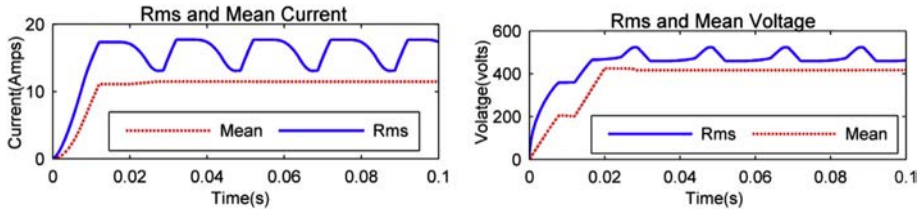

Fig. 5. Current and Voltage waveforms using a DC–DC Buck-Boost converter with controlled converter load.

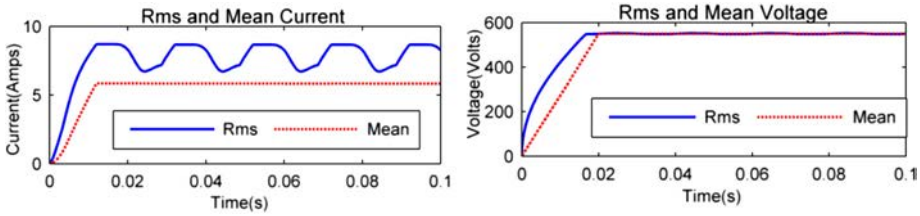

Fig. 6. Current and Voltage waveforms using a DC–DC Buck converter with fully controlled converter load.

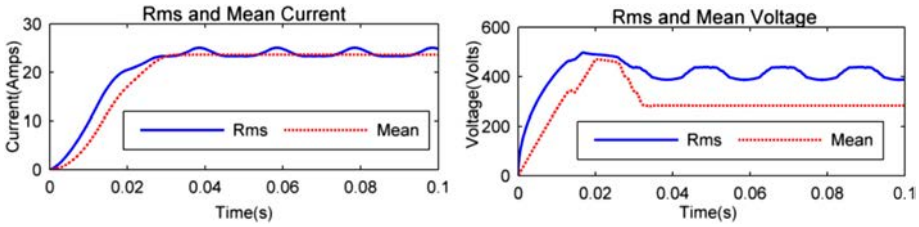

Fig. 7. Current and Voltage waveforms using a DC–DC Boost converter with fully controlled converter load.

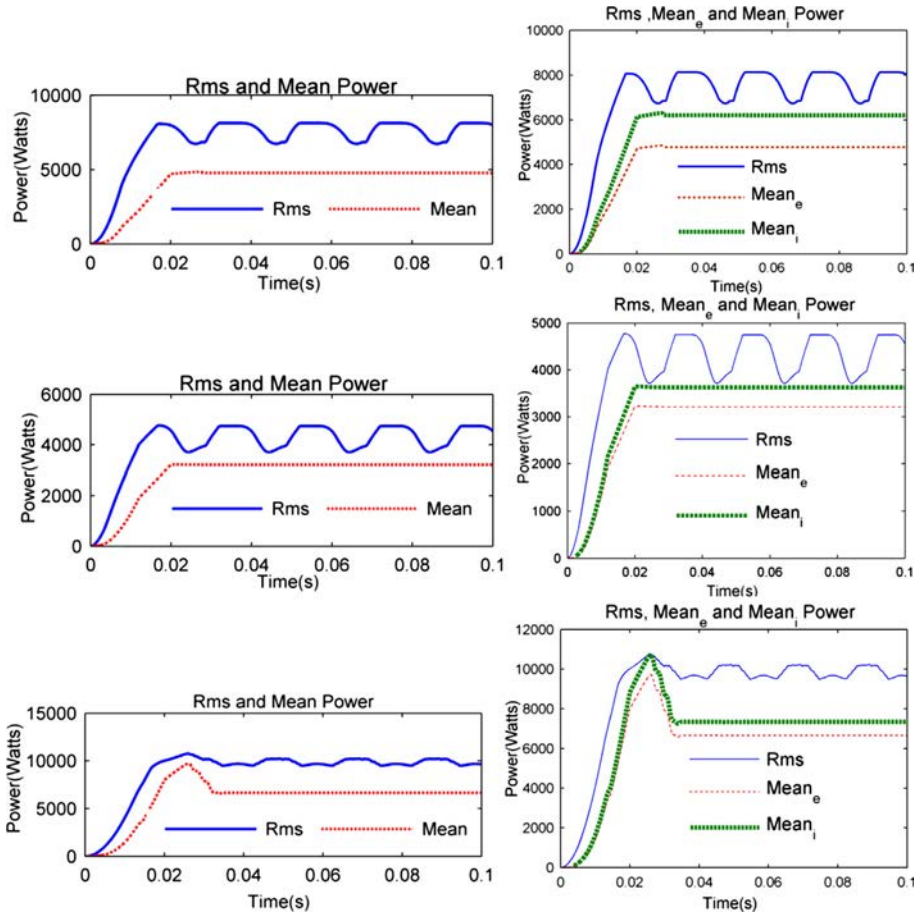

Fig. 8. Output Power waveforms of a DC–DC Buck-Boost converter, DC–DC Buck converter and DC–DC Boost converter with fully controlled converter load with comparison of existing and improved techniques.

4. Simulation results: case 1

A functional model of a photovoltaic panel, general model of a DC–DC converter with incremental conductance MPPT and inverter were used in the simulation done using MATLAB/Simulink. DC–DC Buck, Boost and Buck-Boost converters were simulated for the same load and compared for power variations. The simulation circuit includes a 150 mH inductor and 22 μF capacitors for Buck-Boost converter stage, 5 mH inductor and a 90 μF capacitor for Boost converter stage, 0.5 mH inductor for Buck converter stage. A resistive load of 125 Ω was used for all stages commonly. The system was simulated under controlled and un-controlled converter loads. The MATLAB/Simulink circuit used for simulating the system is shown in Fig. 4. Variations in current, voltage and output power waveforms are provided as a comparative study from Figs. 5–7. Power variations as discussed are certain for changes in the amplitude of current. Adversely varying current leads to power variation which affects the efficency of the MPPT technique.

The result from simulation proves a distinct effect, which a non-linear load has over a PV system with an MPPT technique incorporated under the latter technique's influence. The comparison of result of means output power from system simulation with the improved technique ($Mean_i$) adopted in this paper and mean power

Table 1
Electrical parameters of the PV cell under STP.

Maximum power	$P_{MAX} = 100\ W_P$
Voltage at MPP	$V_{MPP} = 17.8\ V$
Current at MPP	$I_{MPP} = 5.62\ A$
Open circuit voltage	$V_{OC} = 21.8\ V$
Short circuit current	$I_{SC} = 6.2\ A$
Temperature coefficient of I_{SC}	$\alpha = 2.46 \times 10^{-3}\ A/^{\circ}C$

Table 2
Measurement obtained from the simulation of the scaled up model of the experimental setup.

S.No	RMS current (amps)	RMS voltage (volts)	Mean current (amps)	Mean voltage (volts)	RMS power (watts)	Mean power$_{(e)}$ (watts)	Mean power$_{(i)}$ (watts)	Efficiency (existing) (%	Efficiency (improved) (%)
(1)	17.6	443	11.5	416	7796	4790	6200	61.2	78.3
(2)	13.3	511	11.5	416	6796	4790	6200	61.2	78.3
(3)	9	540	6	540	4860	3240	3600	40.8	46.5
(4)	7	540	6	540	3780	3240	3600	40.8	46.5
(5)	26	430	24	290	11,180	6960	7900	89.8	96.6
(6)	24	400	24	290	9600	6960	7900	89.8	96.6

obtained from the current technique (Mean$_e$) are shown in Fig. 8. The improvement in power from simulation using the adopted technique proves effective.

5. Experimental results: case 1

The experiment was based on the basic functional diagram provided in Fig. 1. The electrical parameters of the PV panel used in the experimental setup are shown in Table 1. The experimental results were obtained from the setup including a PV source with DC–DC buck-boost MPPT connected to a PWM inverter feeding a fully controlled converter load. TMDSSOLAREXPKIT, with a solar inverter and a MPPT Boost DC–DC converter, was used for MPPT control and the processor control card TMS320F28035 provided gating signal t1 and t2 for the DC–DC converter. Current transducer LTS 25-NP and voltage transducer LV 25-P observed current and

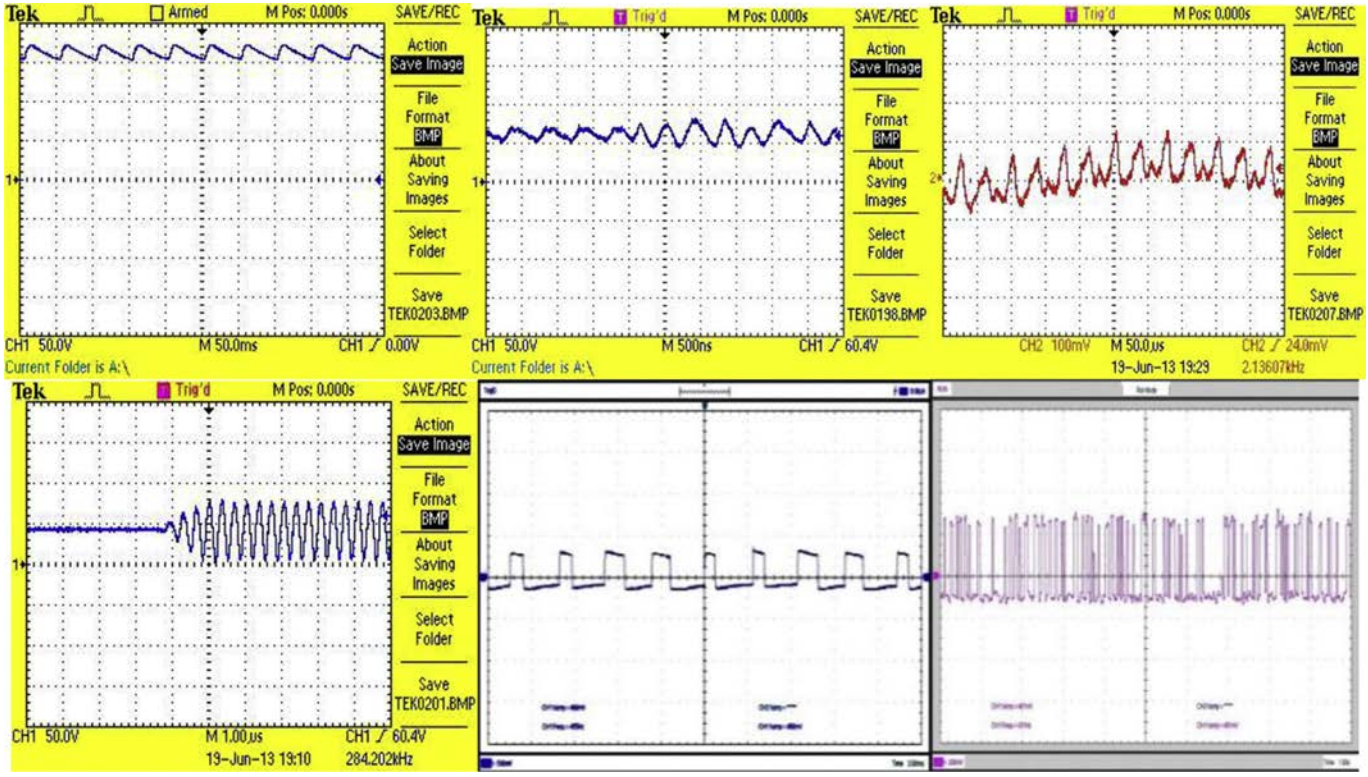

Fig. 9. Experimental measurements scoped.

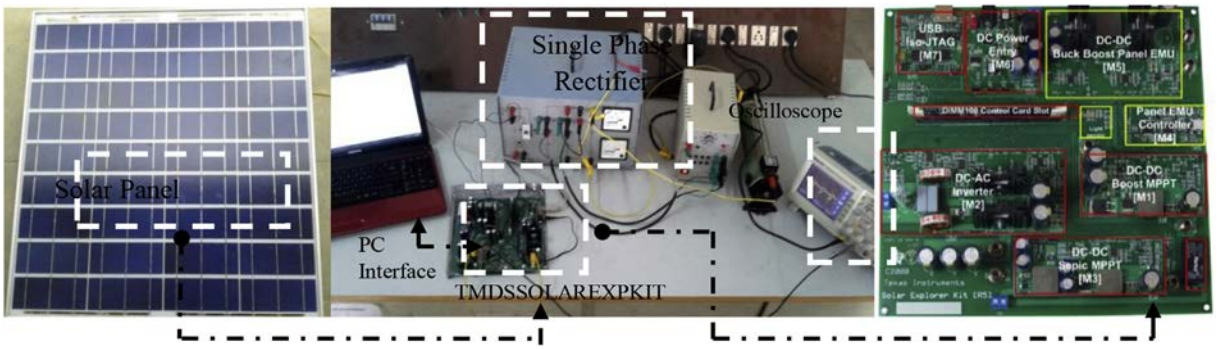

Fig. 10. Experimental hardware setup.

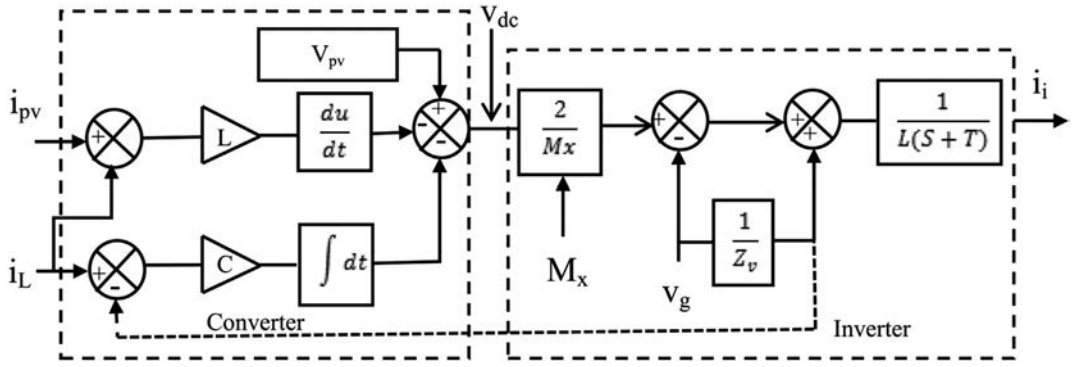

Fig. 11. Simplified model of the PV sourced grid connected inverter.

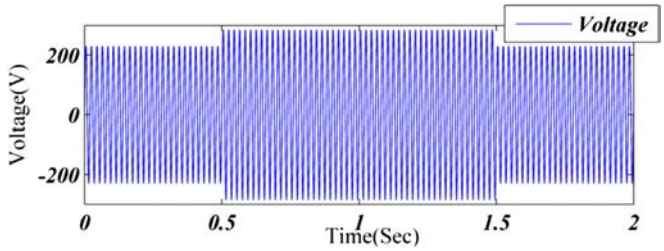

Fig. 12. Voltage Swell waveform.

voltage waveforms in the system. The experimental measurements obtained from the meters, with calculated powers are tabulated in Table 2.

The rows (1 & 2), (3 & 4) and (5 & 6) in Table 2 correspond to the measurements and calculations obtained for the system with DC–DC Buck-Boost, DC–DC Buck and DC–DC Boost converters respectively. The calculations show the difference in RMS Power and Mean Power, which is the reason for reduction in efficiency. The simulation performed is 100 times scaled up to the experimental setup. The improved technique offers a 10 Watt-Hour energy saving for a 100 W_P PV panel, which when calculated for a month's usage (6 h a day) would account for 1.8 kW that is the reason for the reduction in cost of energy consumption. For instance, a 2 kWh saving would result in the reduction of 898 INR for the same calculated duration of utilization based on the tariff of Tamilnadu Generation and Distributed Corporation limited, India (TANGEDCO).

The oscillations found in the current waveforms under different loading conditions are seen in Fig. 9 which explains the difference in power due to the presence of non-linear load under influence of a MPPT technique and the experimental setup used shown Fig. 10.

6. Grid connected PV sourced inverter: case 2

In the second case, the PV sourced inverter is connected with a single phase grid. Fig. 11 shows the simplified model of a grid connected inverter with a PV source. Voltage swell is a common phenomenon in the current power system, the grid over voltage (voltage swell) also affects the power injection of the PV sourced inverter; hence power extracted from PV is not fully pumped up to the grid. This impact creates tremendous energy losses in large PV generating systems. The proposed control technique improves the power injection PV sourced with inverter during voltage swell. The virtual impedance source deducting grid voltage variations is added in the basic model of PV sourced grid connected inverter, through the buck boost converter. The Eq. (14) gives the required dc voltage during a voltage swell

$$V_{dc} = \frac{2}{M_x}\left[V_g + i_1(s)L\left[\frac{R}{L} + S\right] + i_1(s)1/Z_v\right] \tag{14}$$

$$V_{dc} = V_{pv}(sw) \approx LS\left[i_{pv}(s) - i_L(s)\right] - \frac{1}{C_s}\left[i_L(s) - (i_i(s)1/Z_v)\right] \tag{15}$$

7. Simulation result: case 2

As in the first case, simulation was undertaken in MATLAB/Simulink using the functional model of the PV, DC–DC converter with incremental conductance, buck-boost converter and inverter connected with single phase grid. The voltage waveform under swell condition and PV power waveform is obtained for the conventional and improvised incremental conductance MPPT as shown in Figs. 12 and 13.

8. Experimental result: case 2

The same experimental setup of the first case is used here, but the inverter is connected to the single phase grid and PV power variation during overvoltage is observed and recorded. The results of hardware and its 100 times scaled up simulation are tabulated in Table 3 showing variation in the PV power loss in conventional and improvised MPPT techniques. Fig. 14 shows the recorded waveform

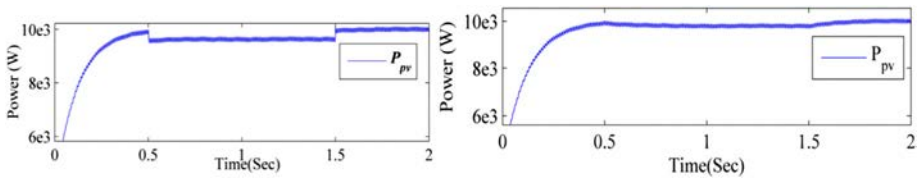

Fig. 13. Waveform of PV Power during swell condition with conventional and proposed MPPT method.

Table 3
Hardware and simulation results of the PV power variation during a voltage swell in the grid.

S. No	Conventional MPPT technique				Improved MPPT technique			
	Hardware result		Simulation result		Hardware result		Simulation result	
	Grid RMS voltage Vg (volts)	PV injected power (watts)	Grid RMS voltage Vg (volts)	PV injected power (watts)	Grid RMS voltage Vg (volts)	PV injected power (watts)	Grid RMS voltage Vg (volts)	PV injected power (watts)
1.	230	97	230	10	230	97	230	10
2.	253	82.45	253	8.53	253	89.24	253	9.35
3.	264.50	77.60	264.50	7.90	264.50	84.39	264.50	8.72
4.	276	72.50	276	7.48	276	79.54	276	8.26
5.	287.50	67.90	287.50	7.0	287.5	74.69	287.50	7.82

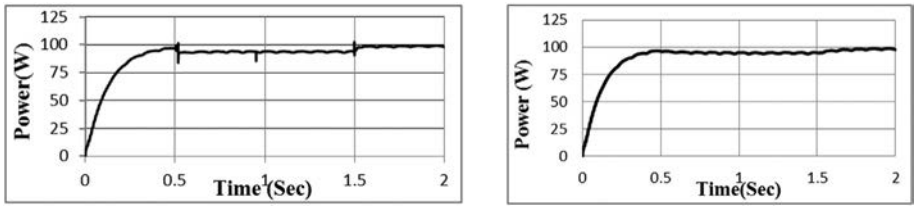

Fig. 14. Hardware results of the PV Power during swell condition with conventional and proposed MPPT method.

of the PV power during a voltage swell condition taken with the conventional and improvised MPPT method.

9. Conclusion

In this paper, the effect of a non-linear load has over the MPPT is analyzed through simulations and a hardware setup. A simple calculation of the panel current as a function of load impedance is introduced in the MPPT algorithm for better results. The simulation of the system was done using MATLAB-Simulink and the hardware setup was created using a TMDSSOLAREXPKIT (Solar explorer kit) for MPPT control. Under non-linear loading conditions, the difference in mean power compared to RMS power was observed due to ripples present in the current waveform under the influence of the MPPT. Simulations and experimental results verify the effects of non-linear loading. The cost efficiency calculation presented shows the profound importance of the analysis in this research. In the second case, the drop in PV power due to a voltage swell is reduced greatly under the proposed MPPT condition, verified from simulation and hardware results.

References

[1] Sahin Arzu Sencan. Modelling and Optimization of Renewable energy systems. May 2012. p. 21–52 [chapter 2].
[2] Djamila Rekioua and Ernest Matagne, Optimization of photovoltaic power systems, Springer, Green energy and technology, [chapter 2]: 53–79.
[3] Patel Hiren, Agarwal Vivek. MATLAB-based modeling to study the effects of partial shading on PV array characteristics. IEEE Trans Energy Convers 2008;23(1):302–10.
[4] Ding Kun, Bian XinGao, Liu HaiHao, Peng Tao. A MATLAB-Simulink-based PV module model and its application under conditions of non-uniform irradiance. IEEE Trans Energy Convers 2012;27(4):864–72.
[5] Liu Fangrui, Duan Shanxu, Liu Fei, Liu Bangyin, Kang Yong. A variable step size INC MPPT method for PV systems. IEEE Trans Industrial Electron 2008;55(7): 2622–8.
[6] Gergaud O, Multon B, Ben ahmed H, Analysis and experimental validation of various photovoltaic system models. Proc 7th Int ELECTRIMACS' 2002 Congr, [Montréal].
[7] Kjær Søren Bækhøj. Evaluation of the hill climbing and the incremental conductance maximum power Point trackers for photovoltaic power systems. IEEE Transactions Energy Convers 2012;27(4):922–9.
[8] De Brito MAG, Galotto L, Sampaio LP, de Azevedo e Melo G. Evaluation of the main MPPT techniques for photovoltaic applications. IEEE Trans Ind Electron 2013;60(3):1156–67.
[9] Subudhiand Bidyadhar, Pradhan Raseswari. A comparative study on maximum power Point tracking techniques for photovoltaic power systems. IEEE Trans Sustain Energy 2013;4:89–98.
[10] Esram Trishan, Chapman Patrick L. Comparison of photovoltaic array maximum power Point tracking techniques. IEEE Trans Energy Conserv 2007;22(2):439–49.
[11] Elgendy, Zahawi B, Atkinson DJ. Assessment of the incremental conductance maximum power Point tracking algorithm. IEEE Trans Sustain Energy January 2013;4(1):108–17.
[12] De Araujo Ribeiro RL, de Azevedo CC, de Sousa RM. A robust adaptive control strategy of active power filters for power-factor correction, harmonic compensation, and balancing of nonlinear loads. IEEE Trans Power Electron 2012;27(2):718–30.
[13] Singh Mukhtiar, Chandra A. Adaptive neuro-fuzzy control of renewable interfacing inverter to maintain smooth power flow and non-linear unbalanced load compensation simultaneously. IEEE Electr Power & Energy Conf 2009:1–6. Montreal, QC.
[14] Umeh KC, Mohamed A, Mohamed R. Determining harmonic characteristics of typical single phase non-linear loads. Student Conf Res Dev 2003:413–9.
[15] Wang Kui, Shuhua Guan, Qian Hou, Yuanhong Hou. Investigation of harmonic distortion and losses in distribution systems with non-linear loads. Int Conf Electr Distribution 2008:1–6. Guangzhou.